Developing skills in Silicon Photonics with Design, Fabrication and Analysis of Interferometers workflow.

Grigorii Vydrevich

July 10, 2025

Abstract

This report details the design, simulation, fabrication, and characterization of Mach-Zehnder Interferometers (MZIs) on a silicon-on-insulator (SOI) platform. Strip waveguides with a nominal cross-section of 500×220 nm^2 were used. The impact of varying path length differences (ΔL) on the MZI's spectral response, specifically the Free Spectral Range (FSR), was investigated through simulation using Lumerical INTERCONNECT and MODE Solutions. Devices will be fabricated using Electron Beam Lithography (EBL). The draft provides the GDS overview of the prepared design. Experimental characterization confirmed the relationship between ΔL and FSR, and extracted group index (n_g) values were compared with simulations, showing good agreement within fabrication tolerances. For instance, for TE mode MZIs, group index errors relative to nominal simulations were typically below 0.5 %.

1 Introduction

Silicon photonics has emerged as a leading platform for photonic integrated circuits (PICs) due to its potential for high-volume, low-cost manufacturing leveraging existing CMOS infrastructure. It enables high-speed, high-integration devices with reduced power consumption, addressing the growing bandwidth demands in optical communications and other fields. The Mach-Zehnder Interferometer (MZI) is a fundamental building block in silicon photonics, widely used in optical modulators, switches, and filters.

The objective of this project is to design, simulate, fabricate, and characterize silicon photonic MZIs with varying path length differences (ΔL) and archetectrural variants. The goal is to understand the relationship between device geometry (ΔL) and spectral characteristics (Free Spectral Range - FSR), and to compare simulation results with experimental data obtained from fabricated devices.

2 Theory

2.1 Waveguide

The operation of an MZI relies on splitting an input light beam into two paths (arms) and then recombining them. Interference occurs at the output due to the phase difference accumulated between the two paths. For an ideal, lossless MZI with a path length difference $\Delta L = L_1 - L_2$, the output intensity I_o relative to the input intensity I_i is given by:

$$\frac{I_o}{I_i} = \frac{1}{2}[1 + \cos(\beta \Delta L)] \tag{1}$$

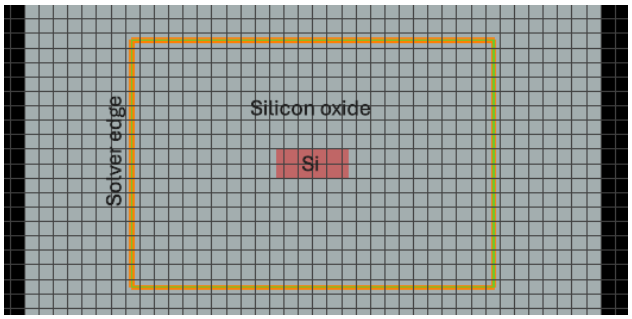

Figure 1: Waveguide representation in Lumerical MODE for physics simulation using FDTD solver

where $\beta = \frac{2\pi n_{eff}}{\lambda}$ is the propagation constant, n_{eff} is the effective index of the waveguide mode, and λ is the wavelength.

The spectral response of an MZI is characterized by its Free Spectral Range (FSR), the wavelength spacing between transmission peaks. The FSR is inversely proportional to the path length difference and the group index (n_g):

$$FSR(\lambda) \approx \frac{\lambda^2}{\Delta L \cdot n_g(\lambda)} \tag{2}$$

where the group index n_g accounts for both material and waveguide dispersion and is defined as:

$$n_g(\lambda) = n_{eff}(\lambda) - \lambda \frac{dn_{eff}(\lambda)}{d\lambda} \tag{3}$$

For simulation purposes, the wavelength-dependent effective index is often approximated using a compact model, such as a Taylor expansion around a central wavelength λ_0 (e.g., 1.55 μm):

$$n_{eff}(\lambda) \approx n_1 + n_2(\lambda - \lambda_0) + n_3(\lambda - \lambda_0)^2 \tag{4}$$

where n_1, n_2, n_3 are fitting coefficients determined from mode simulations. Using Matlab I simulated the data to retrive coefficients $n_{eff}(\lambda) \approx 2.44457 - 1.13036 * (\lambda - 1.55) - 0.0423127 * (\lambda - 1.55)^2$.

2.2 Y-branch

Several components can be used to split or combine optical power in integrated circuits. Common examples used in devices like Mach-Zehnder Interferometers (MZIs) include Y-branches, directional couplers, and Multimode Interferometers (MMIs). Here's a look at Y-branches and related concepts:

2.2.1 Standard Y-Branch

A Y-branch is a simple and common structure used to split power from one input waveguide into two output waveguides, or combine power from two input waveguides into one output waveguide. In MZIs, one Y-branch acts as a splitter (dividing input power equally between the two arms) and another side acts as a combiner. When used as a splitter, an input electric field E_i (corresponding to intensity I_i) ideally splits equally into the two output arms. The fields and intensities in the output arms (E_1, I_1 and E_2, I_2) are:

$$E_1 = E_2 = \frac{E_i}{\sqrt{2}}$$

$$I_1 = I_2 = \frac{I_i}{2}$$

This assumes the split is perfectly symmetric and lossless. When used as a combiner, the input fields E_1 and E_2 from the two arms combine into the output waveguide field E_o:

$$E_o = \frac{E_1 + E_2}{\sqrt{2}}$$

The output intensity I_o depends on the phase difference between E_1 and E_2.

2.2.2 Broadband Directional Coupler

A directional coupler consists of two parallel waveguides brought close enough for their evanescent fields to overlap. This allows power to transfer periodically between the waveguides along the coupling length. By choosing the correct length and gap, a desired splitting ratio (e.g., 50/50) can be achieved at a specific wavelength.

2.2.3 Adiabatic Y-Branch / Adiabatic Splitter

An adiabatic Y-branch (or more generally, an adiabatic splitter) is designed to split power with very low loss and over a broad range of wavelengths by ensuring the transition is extremely gradual. Instead of an abrupt split, the input waveguide slowly transforms into two separate output waveguides, typically with a very small branching angle. The design ensures that the fundamental mode of the input waveguide evolves smoothly (adiabatically) into the lowest-order symmetric mode of the two-waveguide system at the output. This avoids exciting higher-order or radiation modes, minimizing loss. But it requires more space on the chip.

3 Modelling and Simulation

Simulations were performed using Lumerical MODE Solutions for waveguide analysis and Lumerical INTERCONNECT for circuit simulation. MATLAB was used for data fitting and analysis. Furthermore, some analysis steps were developed in Python to match experimental data analysis.

3.1 Waveguide Simulation

Strip waveguides with a silicon core height of 220 nm and various widths (e.g., 400 nm, 500 nm, 600 nm) on an SOI platform with SiO_2 cladding were modeled during the exercises. The standard width used for devices was 500 nm.

Mode analysis was performed to find the effective index (n_{eff}), group index (n_g), and mode profiles for the fundamental quasi-TE and quasi-TM modes across the C-band (1500-1600 nm). Figure 2 shows typical mode profiles. Figure 3 show the simulated n_g versus wavelength for a $500 \times 220\ nm^2$ waveguide.

The compact model coefficients (Eq. 4) were extracted by fitting the $n_{eff}(\lambda)$ data. I also looked at the bending loss depending on the curve radius with $8.5\mu m$ providing less then 0.1%, in our design I use $5\mu m$ as it provides acceptable losses for our design.

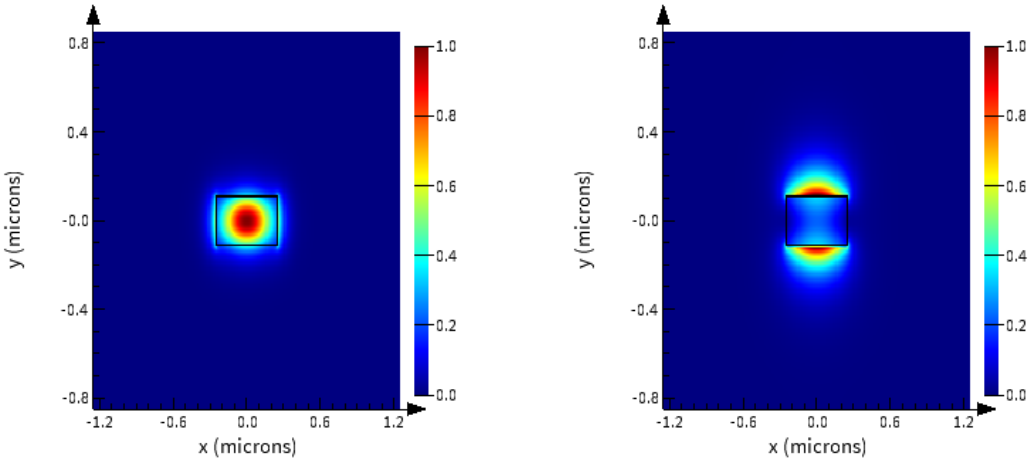

Figure 2: Simulated quasi-TE (left mode 1) and quasi-TM (right mode 2) mode E-intensity profiles for a $500 \times 220\ nm^2$ waveguide at $\lambda = 1550\ nm$.

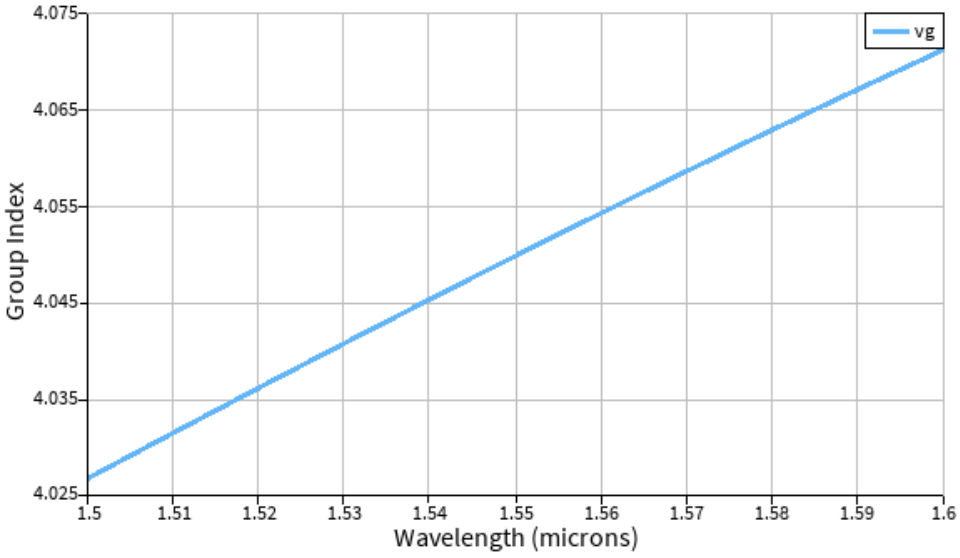

Figure 3: Simulated group index (n_g) vs. wavelength for TE and TM modes in a $500 \times 220\ nm^2$ waveguide.

3.2 Circuit Simulation

MZI circuits were simulated in Lumerical INTERCONNECT 5. The models included grating couplers for input/output coupling and Y-branches for splitting/combining, using provided S-parameter data or models from SiEPIC PDK. Waveguide segments were modeled using the extracted compact models. Simulations were run for various path length differences (ΔL) ranging from 0 μm to over 100 μm.

Figure 4 shows example simulated transmission spectra for MZIs with different ΔL. Expecting, the FSR decreases as ΔL increases.

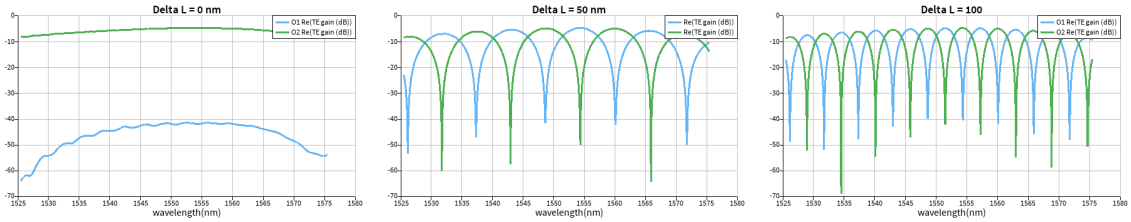

Figure 4: Simulated MZI transmission spectra (TE mode, $500 \times 220\ nm^2$ waveguide) for different path length differences (ΔL).

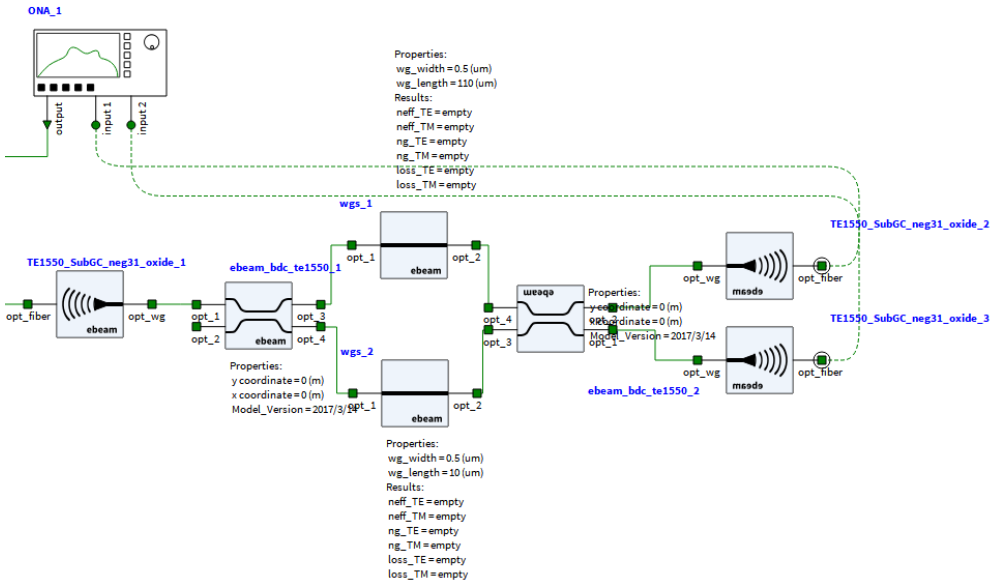

Figure 5: Lumerical INTERCONNECT Mach-Zehnder Interferometer model

4 Physical design

Using SiEPIC PDK I prepared several variations of MZI circut with multiple length differences and different architecture structure to compare the physical differences from the analytical and experimental prospective.

4.1 Layout

The draft layout shows EBeam grigoryvydrevich.oas 8 designs (5 variations of MZIs, 3 Ring variations and a testing device for loss correction). Using KLayout software with SiEPIC extension, the systems were checked for manufacturing compatibility. The main analysis will be carried for MZIs due to the possibility to compare the analytical model with simulation and fabrication data. While Ring models will be compared on variation of the fabrication and simulation.

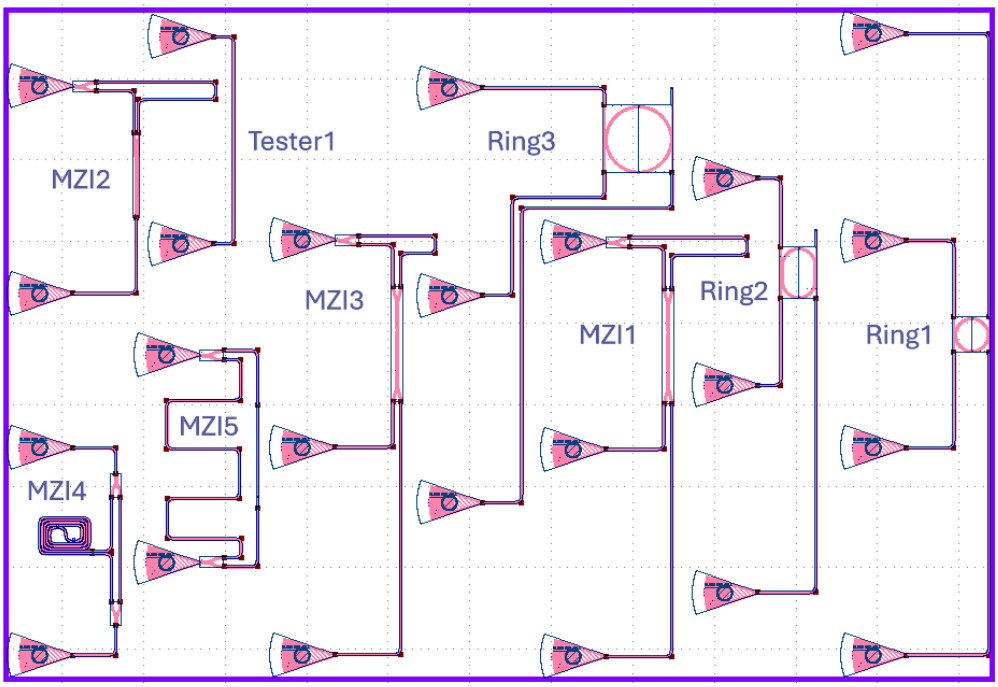

Figure 6: The representation of layout from file. Tester1 - testing device. MZIs ΔL: 1) 100 nm, 2) 100nm, 3) 50 nm, 4) 394 nm 5) 137 nm. Rings: 1) $R = 10, LC = 0$ nm, 2)$R = 10, LC = 10$ nm, 3)$R = 20, LC = 10$ nm

The simulation tools using Monte-Carlo variations give us an idea what could be possible errors and changes in the spectra 7.

4.2 Fabrication

The photonic devices were fabricated using the NanoSOI MPW fabrication process by Applied Nanotools Inc. Edmonton, Canada which is based on direct-write 100 keV electron beam lithography technology.

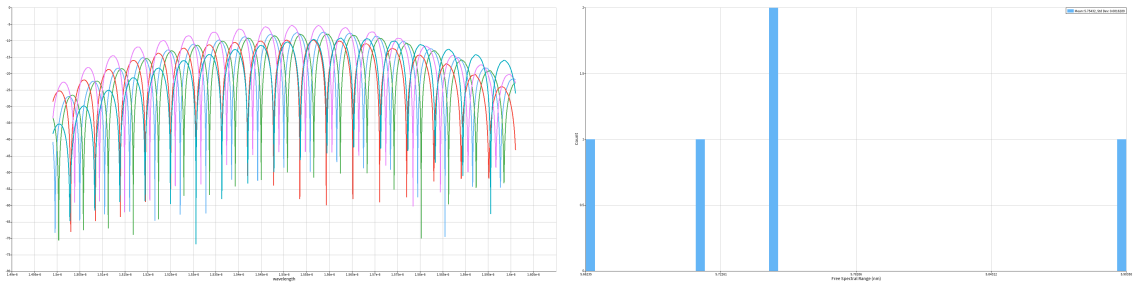

Figure 7: Simulation of variations using Monte-Carlo simulation with Lumerical INTERCONNECT

Silicon-on-insulator wafers of 200 mm diameter, 220 nm device thickness and 2 µm buffer oxide thickness are used as the base material for the fabrication. The wafer was pre-diced into square substrates with dimensions of 25x25 mm, and lines were scribed into the substrate backsides to facilitate easy separation into smaller chips once fabrication was complete. After an initial wafer clean using piranha solution (3:1 H2SO4:H2O2) for 15 minutes and water/IPA rinse, hydrogen silsesquioxane (HSQ) resist was spin-coated onto the substrate and heated to evaporate the solvent. The photonic devices were patterned using a JEOL JBX-8100FS electron beam instrument at The University of British Columbia. The exposure dosage of the design was corrected for proximity effects that result from the backscatter of electrons from exposure of nearby features. Shape writing order was optimized for efficient patterning and minimal beam drift. After the e-beam exposure and subsequent development with a tetramethylammonium sulfate (TMAH) solution, the devices were inspected optically for residues and/or defects. The chips were then mounted on a 4" handle wafer and underwent an anisotropic ICP-RIE etch process using chlorine after qualification of the etch rate. The resist was removed from the surface of the devices using a 10:1 buffer oxide wet etch, and the devices were inspected using a scanning electron microscope (SEM) to verify patterning and etch quality. A 2.2 µm oxide cladding was deposited using a plasma-enhanced chemical vapour deposition (PECVD) process based on tetraethyl orthosilicate (TEOS) at 300^{o}C. Reflectrometry measurements were performed throughout the process to verify the device layer, buffer oxide and cladding thicknesses before delivery.

5 Measurements analysis

To characterize the devices, a custom-built automated test setup [4, 1] with automated control software written in Python was used [3]. An Agilent 81600B tunable laser was used as the input source and Agilent 81635A optical power sensors as the output detectors. The wavelength was swept from 1500 to 1600 nm in 10 pm steps. A polarization maintaining (PM) fibre was used to maintain the polarization state of the light, to couple the TE polarization into the grating couplers [5]. A 90^{o} rotation was used to inject light into the TM grating couplers [5]. A polarization maintaining fibre array was used to couple light in/out of the chip [2]. Raw experimental data includes the transmission spectrum for each device. Figure 9 shows an example of a measured spectrum. Before analysis, the spectrum is typically calibrated by subtracting the wavelength-dependent loss of the grating couplers, often estimated using a polynomial fit to the peaks or by measuring loop-back structures (two connected grating couplers) 8.

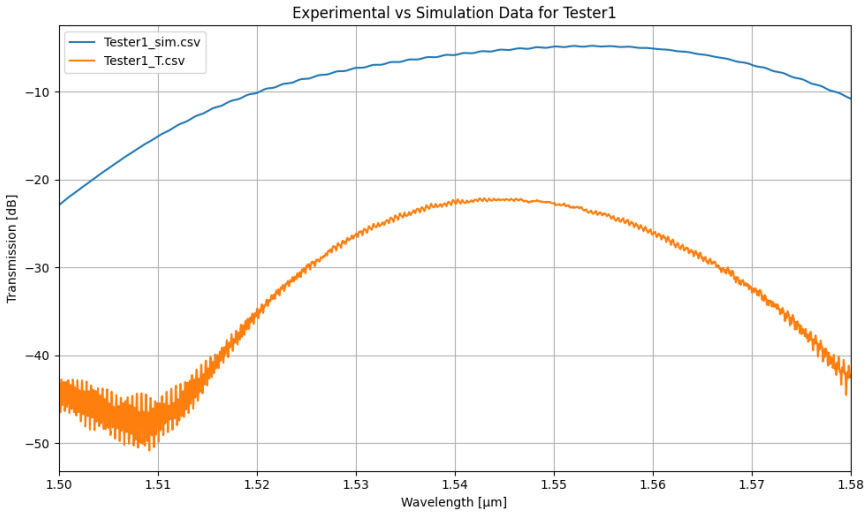

Figure 8: Measured transmission spectrum for simulation and experimental **Tester1**.

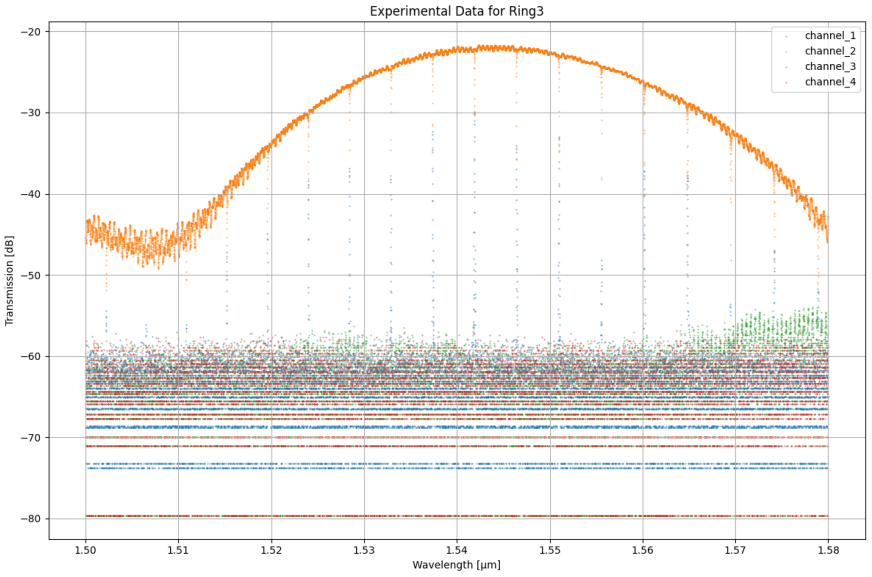

Figure 9: Measured transmission spectrum (main channel - orange) for a TE Ring 3 with radius $R = 20nm$).

5.1 Manufacturing Variability

To assess the impact of fabrication variations, corner analysis was performed for TE polarization. Variations in waveguide width from 500nm (e.g., nominal ±20 nm or +10/-30 nm) and silicon layer thickness (e.g., 220 nm nominal, actual 215.3-223.1 nm were considered. These variations affect n_{eff} and n_g, shifting the device's spectral response. The simulations predict n_g at 1550 nm to be within approximately 4.1587 to 4.2369. Based on the data analysis of the structure, the extracted ng = 4.1630, which falls in the range of accepted tolerance rate.

6 Analysis

Data analysis focused on extracting key parameters like the group index (n_g) from the measured MZI spectra and comparing them to simulations. The FSR was determined from the calibrated spectra by finding peak spacing. Then, n_g was calculated using a rearrangement of Eq. 2: $n_g(\lambda) \approx \frac{\lambda^2}{\Delta L \cdot FSR(\lambda)}$.

Alternatively, the entire measured spectrum can be fitted to a theoretical MZI model (incorporating the compact model Eq. 4 and potentially loss terms) to extract the waveguide parameters (n_1, n_2, n_3, loss α). Figure 10 shows an example fit.

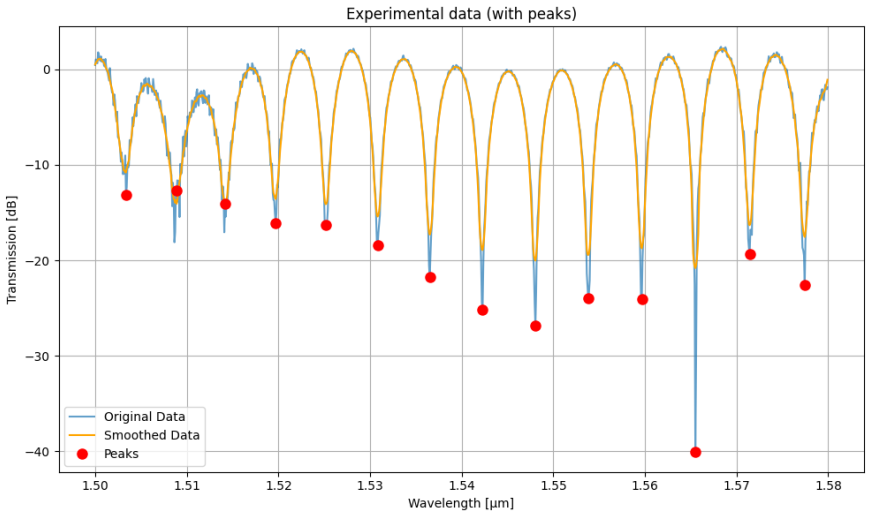

Figure 10: Measured transmission spectrum for a TE MZI1 with $\Delta L \approx 100\ \mu m$ the calibrated experimental data (blue) for an MZI to the theoretical model (orange) to extract parameters. Calculation $n_g = 4.163, FSR = 5.76$ nm.

The experimentally extracted group index was compared to the simulated nominal value and the range predicted by corner analysis. The experimental results generally fall within or close to the predicted range from corner analysis, validating the simulation models and fabrication process characterization. For example, measured n_g values for TE MZIs were often found to be around 4.16-4.23 (for MZI1, MZI2, MZI3, consistent with simulations. Discrepancies can be attributed to the actual fabricated dimensions deviating from the

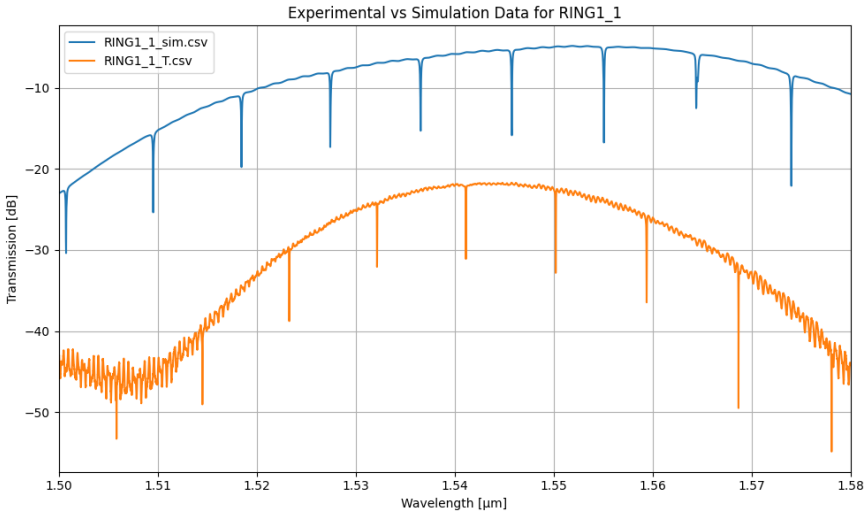

Figure 11: Measured transmission spectrum for a TE Ring1 with Radius = 10 nm.

nominal design.

This also shows in the depth of sharp peaks and smaller oscillations for Ring resonators, which can depend a lot on the fabrication variability 11.

7 Conclusion

This project successfully demonstrated the design, simulation, and characterization of silicon photonic Mach-Zehnder interferometers. The relationship between the path length difference (ΔL) and the Free Spectral Range (FSR) was confirmed both in simulation and experiment. Simulation models using Lumerical tools accurately predicted device behavior. Waveguide parameters, particularly the group index (n_g), were extracted from experimental data and showed good agreement with simulations when fabrication variability (corner analysis) was considered. Typical group index errors compared to nominal simulations were less than 0.5 % for TE modes indicating reasonable predictability of the fabrication process. This work provides a practical example of the silicon photonics design flow from concept to measured results.

Acknowledgements

I acknowledge the edX UBCx Phot1x Silicon Photonics Design, Fabrication and Data Analysis course, which is supported by the Natural Sciences and Engineering Research Council of Canada (NSERC) Silicon Electronic-Photonic Integrated Circuits (SiEPIC) Program. The devices were fabricated by Richard Bojko at the University of Washington Washington Nanofabrication Facility, part of the National Science Foundation's National Nanotechnology Infrastructure Network (NNIN), and Cameron Horvath at Applied Nanotools, Inc. Omid Esmaeeli performed the measurements at The University of British Columbia. I acknowledge Lumerical Solutions, Inc., Mathworks, Mentor Graphics, Python, and KLayout for the design software.

References

[1] Maple leaf photonics. `http://mapleleafphotonics.com`, 2025.

[2] PLC connections. `www.plcconnections.com`, 2025.

[3] Siepic probe station. `http://siepic.ubc.ca/probestation`, 2025. Using Python code developed by Michael Caverley.

[4] Lukas Chrostowski and Michael Hochberg. *Silicon Photonics Design: From Devices to Systems*. Cambridge University Press, 2015.

[5] Yun Wang, Xu Wang, Jonas Flueckiger, Han Yun, Wei Shi, Richard Bojko, Nicolas A. F. Jaeger, and Lukas Chrostowski. Focusing sub-wavelength grating couplers with low back reflections for rapid prototyping of silicon photonic circuits. *Optics Express*, 22:20652–20662, 2014.

Use of AI tools

The work of the project was done with the help of AI tools such as Gemini Flash2.5,ChatGPT for help with the code adaptation and debugging, and Writefull, LanguageTool for report text improvement suggestions as well as Perplexity for further research and resource analysis.

Code availabiltity

The code used for analysis was developed based on the provided scripts for MATLAB and adapted for Python to help with new data formats and better connectivity with fitting tools. It can be used within Google Colab framework or downloaded as Jupyter Notebook - Analysis script